Identification of yttrium oxide-specific peptides for future recycling of rare earth elements from electronic scrap

Maass, D.; Boelens, P.; Bloß, C.; Claus, G.; Harter, S. D.; Günther, D.; Pollmann, K.; Lederer, F.;

Originally published:

January 2024

Biotechnology and Bioengineering 121(2024)3, 1026-1035

DOI: https://doi.org/10.1002/bit.28629

Identification of yttrium oxide-specific peptides for future recycling of rare earth elements from electronic scrap

Danielle Maass[1,*], Peter Boelens[2], Christoph Bloss[2], Gerda Claus[2], Sonja Harter[2], Dominik Günther[2], Katrin Pollmann[2], Franziska Lederer[2,*]

[1] Universidade Federal de São Paulo. Instituto de Ciência e Tecnologia; Departamento de Ciência e Tecnologia, São José dos Campos, SP, Brazil

[2] Helmholtz-Zentrum Dresden-Rossendorf, Helmholtz Institute Freiberg for Resource Technology, 01328 Dresden, Germany

*danielle.maass@unifesp.br; f.lederer@hzdr.de

Conflict of interest statement: The authors declare that there is no conflict of interest.

Data availability statement: Data will be provided when requested.

Abstract

Yttrium is a heavy rare earth element that acquires remarkable characteristics when it is in oxide form and doped with other rare earth elements. Owing to these characteristics Y_2O_3 can be used in the manufacture of several products. However, a supply deficit of this mineral is expected in the coming years, contributing to its price fluctuation. Thus, developing an efficient, cost-effective, and eco-friendly process to recover Y_2O_3 from secondary sources has become necessary. In this study, we used phage surface display to screen peptides with high specificity for Y_2O_3 particles. After three rounds of enrichment, a phage expressing the peptide TRTGCHVPRCNTLS (DM39) from the random pVIII phage peptide library Cys4 was found to bind specifically to Y_2O_3, being 531.6-fold more efficient than the wild-type phage. The phage DM39 contains two arginines in the polar side chains, which may have contributed to the interaction between the mineral targets. Immunofluorescence assays identified that the peptide's affinity was strong for Y_2O_3 and negligible to $LaPO_4$:Ce^{3+},Tb^{3+}. The identification of a peptide with high specificity and affinity for Y_2O_3 provides a potentially new strategic approach to recycle this type of material from secondary sources, especially from electronic scrap.

Keywords: e-waste; mineral binding peptides; next-generation sequencing; phage surface display; waste of electrical and electronic equipment

1. Introduction

Yttrium (Y) is classified as a heavy rare earth element (REE), being closely associated with lanthanides in nature since they tend to occur in the same ore deposits (Mechnich, Braue, 2013). Y presents both ionic radius and ionic charge similar to that of holmium (Ho) and, as the other lanthanide metals, its oxidation state is mainly +3. This type of element is considered indispensable and non-replaceable in many electronic, catalytic, magnetic, and optical applications due to its capacity to accept and discharge electrons (Platt, 2017; Seredin, Dai, 2012; Macheyeki et al., 2020). The applications of this element are numerous, for example as phosphors in fluorescent lamps, it is also used to create cubic zirconia jewels, in fighter jet engines, as wind turbine additives, as laser in industrial, medical, and graphic technologies, in electronic components for missile defense systems, and others (Munisha et al., 2022). When Y is in the oxide form, it is predominantly applied in the nuclear industry, since its melting temperature is well beyond 2400 °C, being used as protection against thermochemical attack by slags, molten metals, etc.

Since 2016, the yttrium oxide price worldwide has been more stable, ranging between US$/kg 3.66 and US$/kg 2.94 (Macheyeki et al., 2020). However, a deficit in the supply of yttrium oxide is expected in the coming years even if the global REE market practically doubles its production by 2030 (Statista Research Department, 2022; Innocenzi et al., 2014). Thus, the possibility of recovering Y from secondary sources such as e-waste may reduce any threat of supply reductions (Zhang et al., 2016).

In the literature, several authors studied the recovery of Y from waste of electrical and electronic equipment (WEEE). For instance, Pan et al. (2013) reported a method to recover Y from waste phosphors of TV screens. The treatment included: roasting with ammonia chloride; dissolution of yttrium chloride with water; purification with sodium sulfide; precipitation with

oxalic acid and calcination at high temperatures. After reacting 1 g of sample with 8 g ammonia chloride for 30 min at 90 ºC, a Y recovery rate of 92% was found. Yan et al. (2016) were able to recover Y from flat panel display waste by washing the waste several times before starting the leaching process with 1 M HCl and 1 M NaOH. The authors extracted the target material using 1 M HCl with 0.25 M Cyanex 923 diluted in kerosene, followed by stripping with 1 M HNO_3 and further purification with 0.2 M DEHPA diluted in kerosene. Furthermore, Kaim et al. (2023) highlighted that Ionic liquids (ILs) are a promising alternative to these organic/volatile solvents methods for selective recovery of Y and other REEs from secondary sources in terms of sustainability and as much as diminishing risks of toxicity and explosion. However, some challenges need to be overcome, *e.g.*, a decrease of some ILs costs, scale-up ILs extraction from real e-waste, and improving reuse and recycling of ILs after the extraction process. As can be noticed, these methods require a high demand for reagents and energy (that exceed the current market prices of Y by far) or are not well developed. In this sense, biotechnological processes can contribute to solving some of these problems since they use natural tools to promote the recovery of metals and REEs, not being energetic or chemically demanding (Pollmann et al., 2018).

Among the biotechnological processes, one attractive approach is the use of peptides that can bind specifically to REEs, increasing their recovery rate by different separation processes. To identify selectively binding peptides, phage surface display (PSD) techniques are used. During the biopanning process, target-selective phage modified with additional peptides are enriched from large phage peptide libraries (Pollmann et al., 2018). During the last decades, PSD has mainly been used in the medical field, especially for the discovery of diagnostic and therapeutic peptides (Kuzmicheva, Belyavskaya, 2017). Currently, the usability of PSD for solid- and inorganic material binding has proven to be successful not only in medicine applications but both in the

nanotechnology and biomining fields (Seker & Demir, 2011, Care et al., 2015, Braun et al., 2018). For instance, Lederer et al. (2017, 2019) screened for peptide sequences that could specifically bind to fluorescent phosphor compounds which are commonly found on compact fluorescent lamps, such as $LaPO_4:Ce^{3+},Tb^{3+}$ (LAP), $CeMgAl_{11}O_{19}:Tb^{3+}$ (CAT), $BaMgAl_{10}O_{17}:Eu^{2+}$ (BAM), and $Y_2O_3:Eu^{3+}$ (YOX). The authors used two random pVIII phage peptide libraries for biopanning assays, being able to find single peptides that strongly bind to almost all target materials, except YOX. Thus, the development of highly specific peptides that bind with high affinity to Y or Y_2O_3 can be very promising in terms of efficiency and sustainability (Innocenzi et al., 2014). In the following work, we aimed to identify and characterize peptides that bind to solid Y_2O_3 using PSD as a key method to develop peptides with high specificity. Peptide sequences that bind selectively to the target material were screened using the random pVIII f88-Cys4 12-mer peptide library. After three rounds of enrichment, phage containing a surface peptide that bound specifically to Y_2O_3 were identified and characterized. Owing to peptides' robust properties and variability in their amino acid sequence, they may be suitable ligands for the biosorptive complexation of Y in solid waste, contributing to Y recovery in the future (Matys et al., 2017).

2. Material and methods

2.1 Bacterial host preparation

In this study, *Escherichia coli* K91 BlueKan (λ− Su− thi Hfr Cavelli) (Bonnycastle et al., 1996; Smith and Scott, 1993) was used for phage amplification. Competent cells were prepared by inoculating a single culture from a pre-prepared minimal agar plate to a tube containing 2 mL of NZY medium, which is composed of 10 g/L of N-Z-Amine A, 5 g/L yeast extract, and 5 g/L of

NaCl. The tube remained overnight in a rotary shaker at 37 ºC and 250 rpm. Then 400 µL of the overnight culture was transferred to a flask containing 20 mL of NZY medium and left in a rotary incubator at 250 rpm, and 37 ºC until they reached the mid-log phase (OD_{600} = 0.45). To allow the cells for F-pili regeneration, the shaking speed was reduced to 100 rpm for 10 minutes. The cells were separated by centrifugation (10 min, 2,200 rpm, 4 ºC) and gently resuspended in 20 mL of 80 mM NaCl. The flask was incubated for 45 min at 37 ºC and 100 rpm. The cells were collected by centrifugation (2,800 rpm, 10 min, 4 ºC) and resuspended in 1 mL NAP buffer (80 mM NaCl, 50 mM $NH_4H_2PO_4$, pH 7.0), remaining stocked at 4 ºC.

2.2 Phage surface display

The target material (Y_2O_3, Merck, 99.9%) was ground using a mortar and pestle, and its primary particle size distribution was determined with a HELOS laser diffraction analyzer (Sympatec GmbH, Clausthal-Zellerfeld, Germany). 20 mg of the ground Y_2O_3 was washed three times with 1 mL of Tris-buffered-saline (TBS, 50 mM Tris-HCl, 150 mM NaCl, pH 7.5), and incubated overnight in an overhead shaker at 4 ºC in 1 mL of phosphate-buffered-saline (PBS, 137 mM NaCl, 2.68 mM KCl, 8.1 mM Na_2HPO_4, 1.47 mM KH_2PO_4, pH 7.4) containing 10 mg/L of bovine serum albumin (BSA). The target material was centrifuged for 1 min at 14,000 rpm, the supernatant was discarded and washed three times with 1 mL TBS.

Biopanning assays were accomplished in three rounds using the random f88-Cys4 12-mer pVIII phage library (from Creative Biolabs, Shirley, NY) according to the manufacturer's instructions. This library is described in more detail in a previous work by Lederer et al. 2017. In the first round, 100 µL of amplified f88-Cys4 library and 900 µL of binding buffer (TBS containing 1% (v/v) Tween-20 and 1 mg/L BSA, pH 8.3) were added in a negative panning to an empty

Eppendorf tube and after one hour of incubation, the supernatant was transferred to the prepared Y_2O_3 target. The microtube remained in an overhead shaker, at room temperature for 1 h, and was then centrifuged at 14,000 rpm for 1 min. The supernatant was separated, and the target was 10-fold washed with TBS containing 0.1% (v/v) of Tween-20 to remove weakly bound phage particles.

Strongly bound phage clones were eluted by the addition of 100 µL of elution buffer (0.1 mM Tris-HCl containing 2 mg/mL BSA (pH 9.1)) and a following incubation on an overhead shaker for 8 min at room temperature. The microtube was centrifuged at 14,000 rpm for 1 min, and the supernatant was transferred to a fresh microtube with 15 µL of neutralization buffer (0.2 M glycine, pH 2.2). The second elution step was done with an additional 100 µL of elution buffer added to the target, vigorously mixed, and spun down at 14,000 rpm for 1 min. The supernatant was transferred to a fresh microtube containing 15 µL of neutralization buffer. The content of both microtubes, entitled eluate, was mixed and submitted to titration. Both input and eluate were diluted and used to infect the host bacteria (*E. coli* K91 BlueKan) to determine the concentration of phage in each case.

The next rounds were accomplished similarly as described above, except that the eluate from each biopanning round was used as the input phage for the next round after being amplified in the bacterial host and purified. The phage concentration from the amplified eluates was adjusted to $2x10^{11}$ cfu. Another change was that the Tween-20 detergent in the binding and washing buffer increased with each successive round of panning to decrease the binding chances of weakly binding phage. The repeating of the cycles was made to enrich the pool of peptide-expressing phage with specific target binding characteristics. After the last biopanning round, random plaques

were picked and placed in 50 µL of TBS, remaining incubated at room temperature for 2 h and were used as the template for PCR amplification and stored at -21 ºC (Lederer et al., 2018).

2.3 Characterization of phage

The randomly selected single phage were analyzed by Sanger Sequencing. For the Sanger Sequencing analysis, 1 µL sample of each cleared supernatant from biopanning rounds was used as a template in a PCR reaction. The primers that were used for identification of the peptide sequences of the individual pVIII Cys4-phage clones had the following sequence: Phage_f88F (forward), 5´-GCTCTAAATCGGGGGAGCT-3´, Phage_f88R (reverse), 5´-CATAAGCTAGCTTAAAAAAAAGCCCGC-3´. The forward primer was used as a sequencing primer as well. Sanger Sequencing analysis was performed by Eurofins Genomics Europe Shared Services GmbH (Ebersberg, Germany).

2.4 Mini-library screen

The competitive binding assay was accomplished using a so-called “mini-library” which was formed by using the phage that appeared more frequently in the Sanger Sequencing analysis after the last biopanning round and amplified individually. The mini-library was built using an equal number of each phage (10^{10}). One round of biopanning was performed with $2x10^{10}$ of the mini-library, then individual phage were randomly picked up and analyzed again by Sanger Sequencing as previously described (Lederer et al., 2017).

2.5 Immunofluorescence

The immunofluorescence assays were conducted using the methodology previously described by Curtis et al. (2017). Briefly, Y_2O_3 particles were blocked overnight, at 4 ºC, with PBS

containing 10 mg/mL BSA, and then washed twice with TBS. The particles were incubated with 10^{10} phage of one individual peptide expressing phage clone, in TBST-0.1% (TBS buffer containing 0.1% Tween-20) with 1 mg/mL BSA for 1 h at room temperature in an overhead shaker. The samples were washed 10-fold with TBST-0.5%, then twice with TBST-0.05%, and split into two different samples. One of the samples was submitted to a chemical elution (as described in item 2.2) and the other was not eluted. The eluate sample of each phage clone was diluted and used to infect the host bacteria (*E. coli* K91 BlueKan) to determine the concentration of phage in each case. The comparison between the Y_2O_3 binding affinity of peptide-expressing phage efficiency and the wild-type was calculated using Equation (1).

$$Y_2O_3 \text{ binding-affinity of individual phage} = \frac{\%\ individual\ phage\ in\ the\ eluate}{\%\ individual\ phage\ in\ the\ no\ eluate} \quad (1)$$

Anti-M13 antibody (1:1000, Sigma-Aldrich Chemie GmbH, Taufkirchen, Germany) mixed with TBST-0.05% and 10 mg/mL BSA were added to Y_2O_3-samples with and without phage elution, remaining incubated overnight at 4 ºC. The samples were washed 3-fold with PBST-0.05% (PBS buffer containing 0.05% Tween-20) and mixed with Alexa Fluor 594 goat anti-rabbit IgG (1:1000, Fisher Scientific, Invitrogen, Burlington, Ontario, Canada) containing 2 mg/mL BSA for 1 h at room temperature, and then washed again 3-fold with PBST-0.05%. The phage-bound minerals were investigated using an Olympus BX43 microscope (Olympus Optical Europe GmbH, Hamburg Germany) equipped with epifluorescence. The samples were analyzed by increasing 40 times the extent of the objective lens (Olympus, UPlanFl Ph2) with an exposure time of 1.0 s, using Alexa 594 filter (594 nm). Images were captured using Olympus Cellsens Standard imaging software. The negative control consisted of Y_2O_3 particles without phage, but both primary and secondary antibodies. For competitive assays, the same protocol described above was conducted,

with the only difference that Y_2O_3 was mixed to $LaPO_4:Ce^{3+},Tb^{3+}$ (LAP) (50:50), trying to mimic a mixture of two competitive components that are commonly found in lamp phosphor powder.

2.6 Determination of zeta potential

The phage (39, 40, and 80) and the wild-type phage were resuspended in TBS to achieve a concentration of 10^{10} cfu. The phages were precipitated by adding 2.5 M of NaCl containing 20 wt% polyethylene glycol (PEG), remaining incubated on ice for 60 min. Then, they were centrifugated (16,000 rpm) for 10 min and separated from the supernatant. Next, the phage were suspended in a 10 mM KCl solution, and the pH was adjusted to 4.0, 5.6, 7.5, 8.3, and 9.1. The pH-dependent zeta potentials were determined by electrophoretic mobility analysis with a Zetasizer Nano ZS (Malvern Panalytical Ltd., Malvern, UK). The analyses were performed at 25 °C and the Smoluchowski model was used to obtain zeta potentials of the phage. Additionally, the zeta potential of the wild-type phage was also measured at pH 2.6 and 3.2 to confirm the positive surface charge at low pH values.

The zeta potential of the ground Y_2O_3 powder was determined by the Electrokinetic Sonic Amplitude (ESA) effect using an Acoustosizer II v3.28 (Colloidal Dynamics LLC., FL, US). 2 g of the Y_2O_3 powder was suspended in 200 mL of a 10 mM KCl solution (i.e., 1.0 wt%). The samples were introduced into the glass sample reservoir and stirred at a rate of 300 rpm. Then, the solution was pumped through the cell at a flow rate of 90 $mL.min^{-1}$ and the pH was adjusted to 6.1, 7.5, 8.3, 9.1, 10, and 10.7 for the zeta potential measurements.

3. Results and discussion

3.1 Isolation of Y_2O_3-specific phage

The commercially available pVIII phage peptide library f88-Cys4 was amplified and used to screen phage-expressing peptide sequences that bind specifically to the target material (i.e. Y_2O_3). This phage library contains a filamentous phage vector f88.4, which displays randomized peptides at the N-terminal of the phage pVIII protein (Lederer et al., 2017). 96 individual plaques were picked following three rounds of biopanning, having their DNA amplified and the sequences of the encoded pVIII genes determined. Out of the 96 sequences, only 36 sequences showed no stop codons and could be analyzed. None of the 36 sequences occurred more than once.

To identify Y_2O_3 selective phage clones, each of the 36 phages was amplified individually and tittered. Equal numbers of each phage clone were mixed in a mini phage library, which was incubated for one biopanning round with the target Y_2O_3. Forty individual colony forming units (phage clones) were analyzed by Sanger sequencing.

The peptide amino acid sequences and their respective functional residues identified after the mini library screen are presented in Table 1. The sequencing results presented 16 different sequences of which 6 sequences occurred with a frequency from 3 to 8. The most frequently occurring peptide sequence was GPNGCSIFDCLGDQ (DM40) which repeated 8-fold.

Table 1. Mini library summary of the amino acid sequences of isolated Y_2O_3 binding peptides.

			Number of functional amino acid residues		
Peptide	Frequency	Sequence*	Basic	Acidic	Hydrophobic
DM40	8/40	GPNGCSIFDCLGDQ	0	2	6
DM39	5/40	TRTGCHVPRCNTLS	3	0	4
DM80	5/40	KDRNCEYQKCSTMI	3	2	2
DM24	3/40	RTYTCGKSLCILLS	2	0	5
DM15	3/40	RMDNCTKIFCLILK	3	1	5
DM95	3/40	NQTACTQTWCDTVT	0	1	2
DM4	1/40	TRQVCTYNKCTKAD	3	1	2
DM10	1/40	TPEPCQDMDCETIW	0	4	5
DM12	1/40	TWPKCNKGRCNENW	3	1	4
DM13	1/40	RVTNCQRADCMNTY	2	1	2
DM22	1/40	HSHQCRLRLCKSVE	5	1	3
DM27	1/40	QTFRCHRRRCDWRV	6	1	3
DM29	1/40	TQESCADKKCMLTQ	2	2	3
DM37	1/40	NQTACTHTWCDTVT	1	1	3
DM43	1/40	TQKACADNNCMLTQ	1	1	4
DM46	1/40	LTNNCHHKPCPDYS	1	3	3

*Green, nonpolar and aliphatic amino acids; blue, uncharged polar amino acids; black, aromatic amino acids; red, negatively charged amino acids; purple, positively charged amino acids. One sequence contained a stop codon and two sequences were mixtures of several sequences.

For this screen, most of the phage selected contain great portions of polar amino acid side chains followed by apolar or positive charges (see Table 1). Curtis et al. (2009) and Lederer et al. (2017) discussed that although the exact nature of the peptide-mineral interaction is unknown so far, some of the mineral-binding phage sequences seem to be beneficial. According to Curtis et al. (2009), the presence of oxygen and nitrogen in the polar side chains is probably involved in binding with the mineral's inorganic surface. Several peptide sequences in the mini library have oxygen

atoms in their side chains (see Table 1). Oxygen atoms can bind to Y_2O_3 in two ways: (i) monodentate (one amino acid-O binds to Y and the other through an H-bond to a surface-O) bonded conformations on the surface; (ii) bidentate (two format-O's bind to the same Y). An example of this can be seen in Equation (2) (Pedersen & Ojamäe, 2006), where it is possible to observe how formic acid binds to Y_2O_3 particles in an aqueous solution.

$$Y_{12}O_{18}\text{-}(H_2O)_6 + x\text{HCOOH} \rightarrow Y_{12}O_{18}\text{-}(H_2O)_{6\text{-}x}\text{-}(\text{HCOO,H})x + xH_2O \quad (2)$$

Where x is 1, 3, or 6.

However, several studies showed that peptide-mineral binding depends not only on the functional groups of the amino acids but also on the conformation that the peptide adopts and the amino acids arrangement (Curtis et al., 2017; Curtis et al., 2013; Oren et al., 2005; Sarikaya et al., 2004).

3.2 Zeta potential characterization of phage and mineral

To elucidate the mechanisms of peptide-mineral binding, it is necessary to consider that the selective binding of peptides occurs in an aqueous solution, which makes the process even more complex (Curtis et al., 2017). In this sense, some characteristics of Y_2O_3 powder were determined. This mineral had a median grain size diameter, d_{50}, of 1.97 ± 0.08 µm (see Figure 1(a)) and a net positive charge at pH 8.3 (the pH of the binding and washing buffers), presenting a zeta potential of +8.9 ± 3.7 mV (see Figure 1(b)). On the other hand, phage presented a net negative charge since the pH used in the biopanning was above their isoelectric point (~ 4.0) (Tierney; Atema, 1988). The zeta potentials of the samples for pH 8.3 were -20.1, -29.5, -36.2, and -40.0 mV for wild-type, phage DM39, phage DM40, and phage DM80, respectively (see Figure 1(b)). This negative charge probably helped in electrostatic interactions with the positively charged

mineral. Phage DM15, DM24, and DM80 contain one arginine that will be mostly protonated at the pH of the binding and washing buffers (pH 8.3), since its pKa value is 12.48, therefore resulting in a more polar peptide. Phage DM39 contains two arginines, which improves, even more, the negative character of this phage. The presence of two and three lysine residues on the phage DM15 and DM24, respectively, can also increase their electrostatic interactions with Y_2O_3 since the lysine is also mostly protonated in the binding buffer pH, i.e. 8.3.

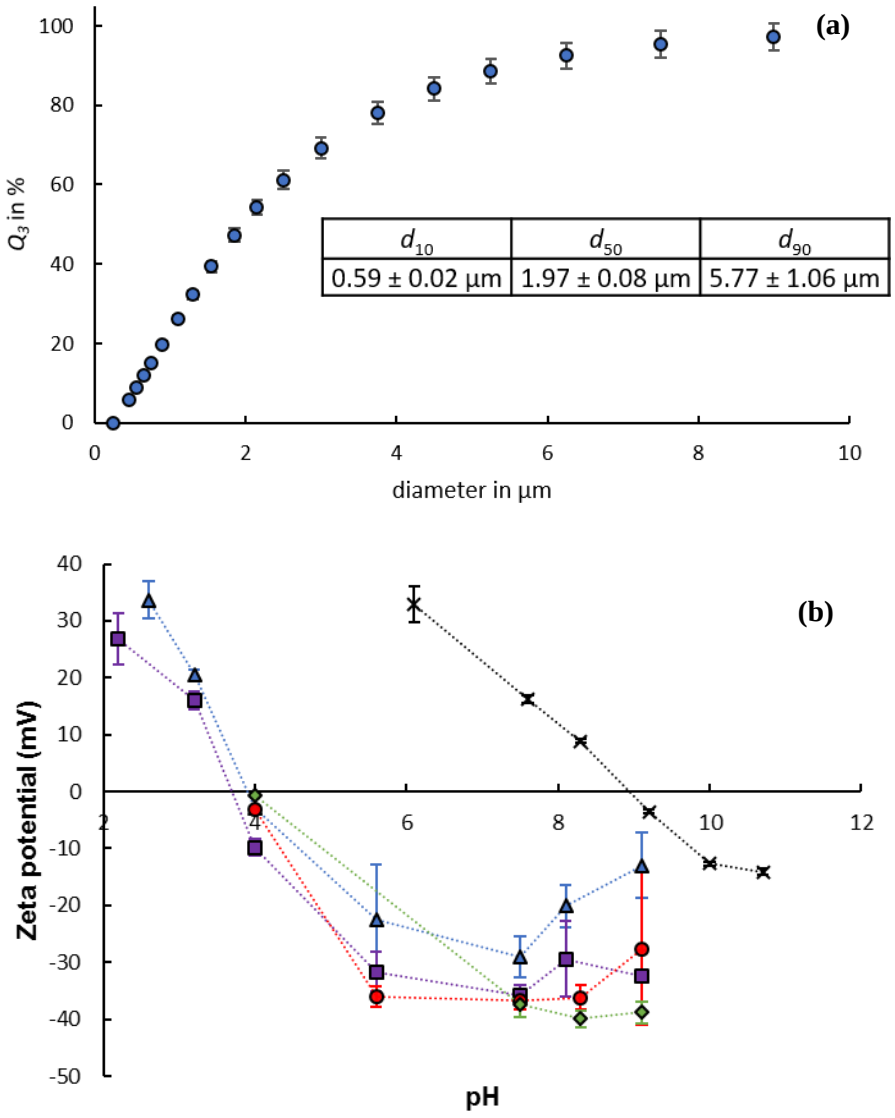

Figure 1. (a) Y_2O_3 size distribution and (b) pH-dependent zeta potential of (x) Y_2O_3 and phage clones (▲wild-type; ■ DM39; ● DM40; ♦ DM80).

The knowledge about phage-mineral electrostatic interactions obtained in this study helped to improve the standard methodology of phage elution commonly used during PSD experiments. Previous studies of PSD with yttrium oxide in this group were not successful (unpublished data) since they used binding and washing buffers with a pH value of 7.5, which may help the phages

to have a more net positive charge. Another point of the standard methodology that was solved was the elution step. Usually, acid elution is capable of releasing phages containing basic amino acids (Bassindale et al., 2007). However, as Y_2O_3 has a net positive charge between pH 6.0-9.0, and the selected phage clones were negatively charged at these pH values, acid elution was not effective in separating the binding peptides from the mineral target. Thus, we used an elution buffer (0.1 mM Tris-HCl and 2 mg/mL BSA) with a pH value of 9.1, obtaining then the elution of the strongly bound phages since Y_2O_3 isoelectric point occurs at pH 9.1 (see Figure 1(b)).

3.3 Comparison between Y_2O_3 binding-affinity of peptide-expressing phage efficiency and the wild-type

After screening the mini-library, the six most frequently occurring phage (see Table 1) were used for individual binding experiments to test which of these phage could specifically bind to Y_2O_3, and the binding affinity was calculated using Equation (1). The phage expressing the peptide TRTGCHVPRCNTLS (DM39) was 531.6-fold more effective in binding to the mineral target than the wild-type phage (see Figure 2). The other phage were less effective in binding to Y_2O_3 than the wild-type phage (0.2–14.3-fold range), clearly showing that the frequency in which the phage appeared did not reflect their binding strength.

Lederer et al. (2017) highlighted that differences in target-binding efficiency can be attributed to the variability in the number of expressed-binding peptides on the phage envelope. That is one of the main advantages of using the pVIII library since it has an increased level of random peptide expression, which can vary from 1% to 10% of pVIII-fusion proteins per phage, i.e., ~40–400 copies per phage, depending on the sequence of amino acids displayed (Curtis et al., 2017). This characteristic of sparse production of recombinant random peptides by the vector

present in the pVIII library allows a more precise separation of peptides that can strongly bind to the target material (Bonnycastle et al. 1996; Lederer et al. 2017).

The loss of function of some phage may also be associated with an effect on multiplication, i.e., the phage with a high propagation rate has an advantage. This behavior is a result of the introduction of bias in the library since changes in the peptide composition and motif frequency occur every time the phages are amplified in *E. coli* host cells (Bakhshinejad et al. 2016). The relation between frequency and strength can be affected due to the loss of a small number of particles during the consecutive washing steps (Lederer et al. 2017), or due to the phage clone adsorption to plastic surfaces or albumin, which is not so easy to prevent (Menendez, Scott, 2005; Vodnik et al., 2011).

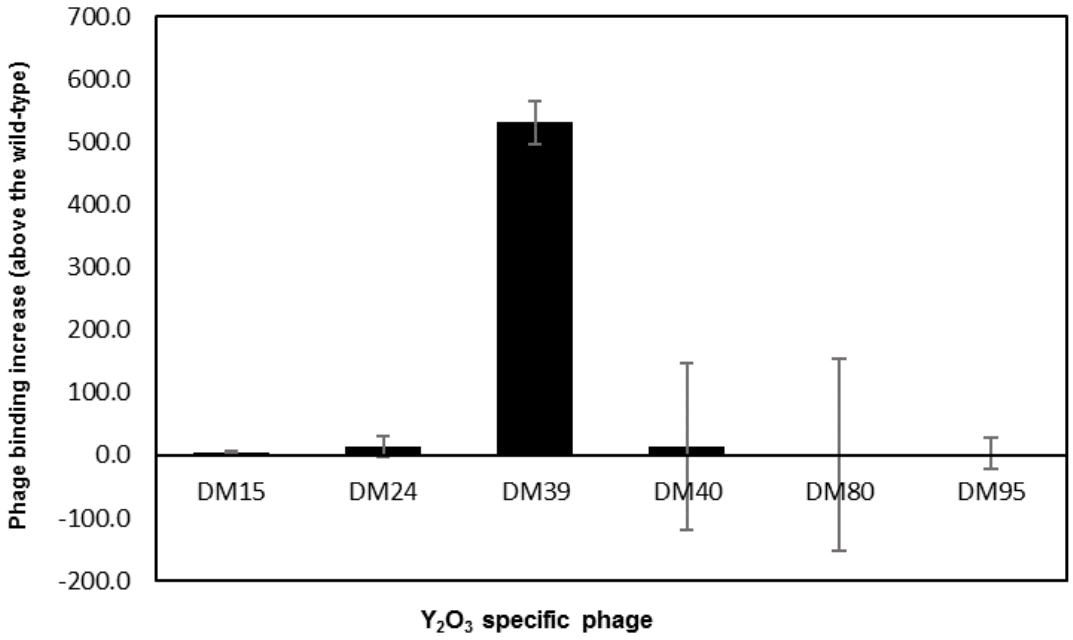

Figure 2. Binding of selected peptide-expressing phage to Y_2O_3. Data are expressed as the fold increase above the percent bound of the wild-type phage from up to three independent experiments.

Data were normalized considering the wild-type phage binding equal to 1 (wt = 1). Error bars represent the standard error.

It is well known that glycine (G) and proline (P) act as secondary structure breakers at any location in the tertiary protein structure (Imai & Mitaku, 2005). Thus, the presence of these amino acids on the polar side of the best binder (DM39) may have influenced the interaction with the mineral particles since these residues do not prefer the interface with the aqueous phase and they enhance the occurrence of disordered structures. Similarly, the presence of amino acids with amphiphilic side chains (such as arginine (R) and histidine (H)) may have increased the disordered regions and consequently increased the hydrophobic character of the phage. Interestingly, the presence of serine (S) and threonine (T) residues on the peptide termini (DM39) may have caused a structural change from a defined secondary structure to a loop due to their entropy effect and flexibility improving the affinity with the target (Imai & Mitaku, 2005).

The difference in the phage's efficiency between phage DM39 and the wild-type was confirmed by immunofluorescence results. It is possible to observe the presence of DM39 phage (red points of light) in the mineral before (Figure 3 (b)) and after chemical elution (Figure 3 (d)). In the assay using only the wild-type, the presence of phage on the target material was not observed (Figure 3 (f) and (g)). The phage DM39 remained bound to the mineral even after elution, meaning that this phage can be defined as a "super-binder" since it presents a very high and resistant affinity to Y_2O_3 (Braun et al., 2018).

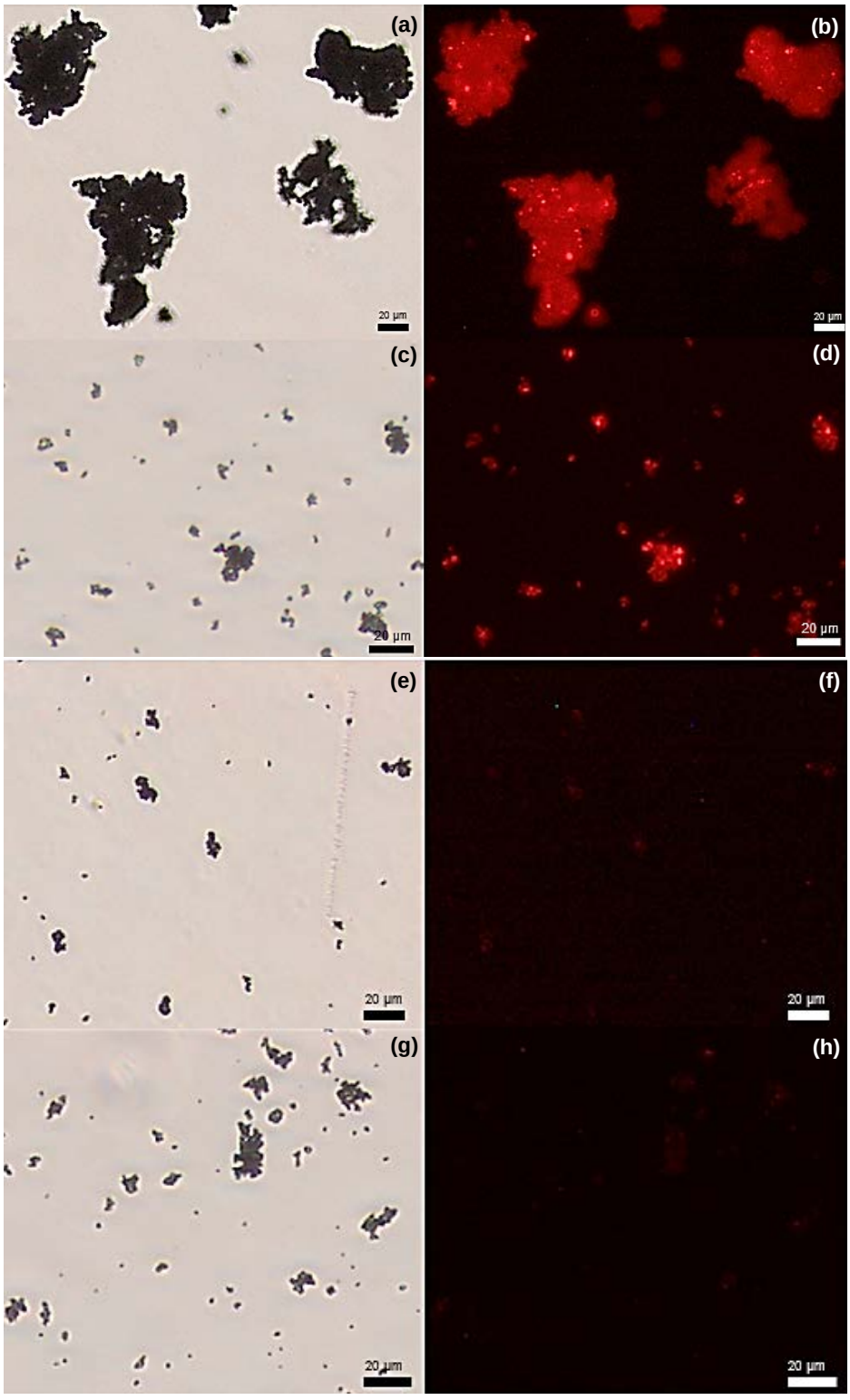

Figure 3. Qualitative binding efficiency of phage DM39 and wild-type phage to Y_2O_3. a, c, e, and g: a light microscope image of yttrium oxide particles. b, d, f, and h: a fluorescent microscopic

images of the same field respectively showing the DM39 phage before (b) and (d) after elution, and wild-type phage before (f) and after elution (h), bound to Y_2O_3. Due to the presence of Alexa Fluor 594 goat anti-rabbit IgG, the phage that are bound to the mineral target appear as red points of light.

3.4 Specificity of phage clone for Y_2O_3

Aiming to use the peptide sequence TRTGCHVPRCNTLS (DM39) for future industrial purposes, we used a mixture of Y_2O_3 and LAP (50:50 weight ratio). The Y_2O_3 characterized in this study and LAP have a similar particle size (Boelens et al. 2021), but opposite surface charge (Boelens et al. 2022). Fluorescence images demonstrate the specificity of the phage DM39 for Y_2O_3 in competition with LAP (see Figure 4) since this phage clone is predominantly bound to Y_2O_3 particles (bound phage clones are the red points of light). It is interesting to note that several previous works by our group had complementary results to these. For instance, Lederer et al. (2017) identified the peptide sequence RCQYPLCS (from the LX-4 pVIII library) which was capable of selectively binding to LAP and not to Y_2O_3. Similarly, Braun et al. (2018) found three peptides that were good binders for LAP, BAM, and CAT, and none of them were good binders for Y_2O_3. Although the complex structure of these minerals needs to be considered, the screening of an Y_2O_3 super-binder from the pVIII library may be attributed to the change in the chemical elution methodology, as discussed in section 3.1.

Further investigations concerning the elucidation of the molecular interactions involved in the phage mineral interaction(s) will be required to improve binding affinity and pave the way to biotechnological solutions for REE recovery. Moreover, it will be interesting to demonstrate that the best binder peptide can be produced by heterologous expression and to investigate if its specificity and efficiency will be maintained. Also, further characterization is needed to quantify

process conditions, reusability, and scale-up possibilities. Furthermore, the peptides identified in this work may be used in the selective separation of Y_2O_3, using superparamagnetic particles (such as Dynabeads) functionalized with surface-binding peptides that can bind to the particles of the target material, facilitating their separation (Boelens et al. 2021; 2022).

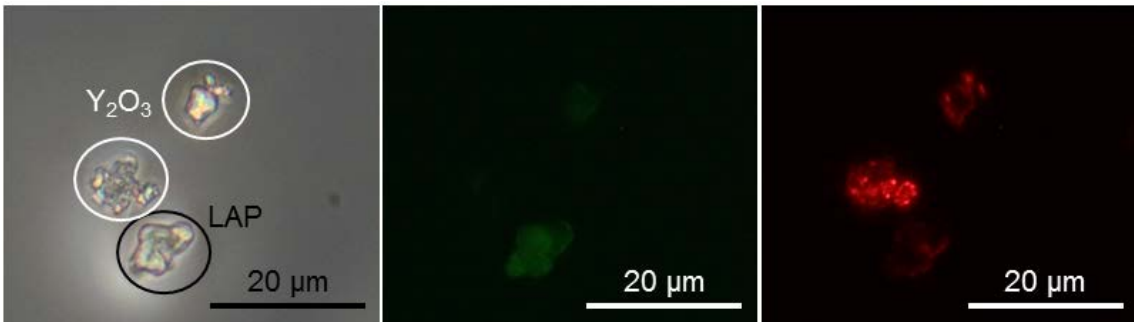

Figure 4. Specific binding of phage expressing the peptide sequence TRTGCHVPRCNTLS (DM39) to a mixture of Y_2O_3 and LAP (50:50) particles: (a) light microscope image of mixed minerals particles; (b) fluorescent microscope image of the same field showing the green fluorescent LAP particles; (c) fluorescent microscope image of the same field showing the DM39 phage bound to Y_2O_3 particles and not to LAP. The phage bound to mineral particles appear as red points of light.

Although this technology still needs to be better developed, it may represent a good opportunity for countries that consume a high amount of yttrium oxide but are totally dependent on importing it from the Chinese market. For instance, both Europe and the U.S.A. have practically a full industrial dependency on China's yttrium, with a rate reaching 100%. That dependency makes yttrium to be currently considered as a critical material. In this sense, developing a technology in which yttrium oxide can be recovered from the internal waste available in those

countries can be very interesting in a medium to long-term period (Charalampides et al., 2015; Zhang et al., 2017).

4. Conclusions

Six phage expressing specific peptides that bind to Y_2O_3 particles were identified. Between them, TRTGCHVPRCNTLS (DM39) was the one that demonstrated the strongest affinity for the target material, being considered a super-binder. Immunofluorescence experiments also demonstrate that DM39 is highly specific for Y_2O_3 binding in competition with LAP. However, a deeper investigation of the molecular interactions involved in the phage-mineral interaction needs to be done. In future studies, the binding behavior of the chemically synthesized peptide TRTGCHVPRCNTLS without any additional phage characteristics will be tested. In the case of effective peptide-mineral interaction, the ability of this unique peptide to mediate the separation of Y_2O_3 from electronic scrap can be a more efficient, cost-effective, and eco-friendly alternative to traditional mineral processing methods.

Acknowledgments

Danielle Maass is thankful to São Paulo Research Foundation (FAPESP) for research grant #2022/09934-5. The team of researchers at HZDR thanks the Sparkassenstiftung “Umwelt und neue Energien” for financial support for consumables needed for this study. The authors would like to thank Sohyun Ahn (Helmholtz Institute Freiberg for Resource Technology, Department of Processing) for her much-appreciated help with the laser diffraction analysis for the determination

of the particle size distribution and her support with the ESA for the zeta potential investigations of Y_2O_3.

References

Bakhshinejad, B., Zade, H. M., Shekarabi, H. S. Z., Mehroke, J. S., Rashed, M., Gong, X., & Scott, J. K. (2016). Phage display biopanning and isolation of target-unrelated peptides: in search of nonspecific binders hidden in a combinatorial library. *Amino Acids, 48,* 2699–2716. *doi*:10.1007/s00726-016-2329-6

Bassindale, A. R., Codina-Barrios, A., Frascione, N., & Taylor, P. G. (2007). An improved phage display methodology of inorganic nanoparticle fabrication. *Chemical Communications,* 2956–2958. *doi*:10.1039/B702650A

Boelens, P., Bobeth, C., Hinman, N., Weiss, S., Zhou, S., Vogel, M., Drobot, B., Azzam, S. S. A., Pollmann, K., & Lederer, F. (2022). Peptide functionalized Dynabeads for the magnetic carrier separation of rare-earth fluorescent lamp phosphors. *Journal of Magnetism and Magnetic Materials, 563,* 169956. *doi*:10.1016/j.jmmm.2022.169956.

Boelens, P., Lei, Z., Drobot, B., Rudolph, M., Li, Z., Franzreb, M., Eckert, K., & Lederer, F. (2021). High-gradient magnetic separation of compact fluorescent lamp phosphors: elucidation of the removal dynamics in a rotary permanent magnet separator. *Minerals, 11,* 1116. *doi*:10.3390/min11101116

Bonnycastle, L. L. C., Mehroke, J. S., Rashed, M., Gong, X., & Scott, J. K. (1996). Probing the basis of antibody reactivity with a panel of constrained peptide libraries displayed by filamentous phage. *Journal of Molecular Biology, 258*(5), 747–762. *doi*:10.1006/jmbi.1996.0284

Braun, R., Bachmann, S., Schönberger, N., Matys, S., Lederer, F., & Pollmann, K. (2018). Peptides as Biosorbents – Promising tools for Resource Recovery. *Research in Microbiology*. *doi*:10.1016/j.resmic.2018.06.001.

Care, A., Bergquist, P. L., & Sunna, A. (2015). Solid-binding peptides: smart tools for nanobiotechnology. *Trends in Biotechnology*, *33*, 259–268. *doi*: 10.1016/j.tibtech.2015.02.005

Charalampides, G., Vatalis, K. I., Apostoplos, B., & Ploutarch-Nikolas, B. (2015). Rare Earth Elements: Industrial Applications and Economic Dependency of Europe. *Procedia Economics and Finance, 24*, 126-135. *doi:*10.1016/S2212-5671(15)00630-9.

Curtis, S. B., Dunbar, W. S., & MacGillivray, R. T. (2013). Bacteriophage-induced aggregation of oil sands tailings. *Biotechnology and Bioengineering, 110*, 803-811. *doi*:10.1002/bit.24745

Curtis, S. B., Hewitt, J., MacGillivray, R. T. A., & Dunbar, W. S. (2009). Biomining with bacteriophage: Selectivity of displayed peptides for naturally occurring sphalerite and chalcopyrite. *Biotechnology and Bioengineering, 102*, 644-650. *doi*:10.1002/bit.22073

Curtis, S. B., Lederer, F. L., Dunbar, W. S., & MacGillivray, R. T. A. (2017). Identification of mineral-binding peptides that discriminate between chalcopyrite and enargite. *Biotechnology and Bioengineering, 114*, 998-1005. *doi*:10.1002/bit.26218

George, G., Senthil, T., Luo, Z., & Anandhan, S. (2021). 22 - Sol-gel electrospinning of diverse ceramic nanofibers and their potential applications. Editors: Dong, Y., Baji, A., Ramakrishna, S.

In: *Woodhead publishing series in composites science and engineering, electrospun polymers and composites, woodhead publishing*, 689-764. *doi:*10.1016/B978-0-12-819611-3.00022-4

Imai, K., & Mitaku, S. (2005). Mechanisms of secondary structure breakers in soluble proteins. *Biophysics (Nagoya-shi), 1*, 55-65. *doi*:10.2142/biophysics.1.55.

Innocenzi, V., De Michelis, I., Kopacek, B., & Vegliò, F. (2014). Yttrium recovery from primary and secondary sources: A review of main hydrometallurgical processes. *Waste Management*, *34*:7, 1237-1250. *doi*:10.1016/j.wasman.2014.02.010

Kaim, V., Rintala, J., & He, C. (2023). Selective recovery of rare earth elements from e-waste via ionic liquid extraction: A review. *Separation and Purification Technology, 306*, Part B, 122699. *doi:*10.1016/j.seppur.2022.122699.

Kuzmicheva, G. A., & Belyavskaya, V.A. (2017). Peptide phage display in biotechnology and biomedicine. *Biochemistry (Moscow), Supplement Series B: Biomedical Chemistry, 11*, 1–15. *doi*: 10.1134/S1990750817010061

Lederer, F. L., Curtis, S. B., Bachmann, S., Dunbar, W. S., & MacGillivray, R.T. (2017). Identification of lanthanum-specific peptides for future recycling of rare earth elements from compact fluorescent lamps. *Biotechnology and Bioengineering*, *114*(5), 1016-1024. *doi*:10.1002/bit.26240

Lederer, F.L., Braun, R., Schöne, L.M., & Pollmann, K. (2019). Identification of peptides as alternative recycling tools via phage surface display – How biology supports Geosciences. *Minerals Engineering*, *132*, 245-250. *doi:* 10.1016/j.mineng.2018.12.010

Macheyeki, A. S., Li, X., Kafumu, D. P., & Yuan, F. (2020). Chapter 2 - Types of ore deposits and their origin. *Applied Geochemistry. Amsterdam: Elsevier*, 45-85. *doi*:10.1016/B978-0-12-819495-9.00002-5

Matys, S., Lederer, F., Schönberger, N., Braun, R., Lehmann, F., Flemming, K., Bachmann, S., Curtis, S., Macgillivray, R., & Pollmann, K. (2017). Phage display - a promising tool for the recovery of valuable metals from primary and secondary resources. *Solid State Phenomena, 262*, 443-446. *doi*:10.4028/www.scientific.net/SSP.262.443

Mechnich, P., & Braue, W. (2013). Air plasma-sprayed Y_2O_3 coatings for Al_2O_3/Al_2O_3 ceramic matrix composites. *Journal of the European Ceramic Society*, *33*:13–14, 2645-2653. *doi:*10.1016/j.jeurceramsoc.2013.03.034

Menendez, A., & Scott, J.K. (2005). The nature of target-unrelated peptides recovered in the screening of phage-displayed random peptide libraries with antibodies. *Analytical Biochemistry, 15*, 145-157. *doi*: 10.1016/j.ab.2004.09.048. PMID: 15620878.

Munisha, B., Mishra, B., & Nanda, J. (2022). Hexagonal yttrium manganite: A review on synthesis methods, physical properties and applications. *Journal of Rare Earths*, *41*:1, 19-31. *doi:*10.1016/j.jre.2022.03.017.

Oren, E. E., Tamerler, C., & Sarikaya, M. (2005). Metal recognition of septapeptides via polypod molecular architecture. *Nano Letters*, *5*(3), 415-9. *doi*:10.1021/nl048425x

Pan, X., Peng, L., Chen, W., Wang, J., & Chen, Z. (2013). Recovery of Y and Eu from waste phosphors of CRT TVs and the preparation of yttrium europium oxide. *Royal Society Chemistry Advances, 9*(3), 1378-1386. *doi:*10.1039/c8ra08158a

Pedersen, H., & Ojamäe, L. (2006). Towards biocompatibility of RE_2O_3 nanocrystals - water and organic molecules chemisorbed on Gd_2O_3 and Y_2O_3 nanocrystals studied by quantum-chemical computations. *Nano Letters, 6*(9), 2004-2008. *doi:*10.1021/nl061185w.

Platt, A. W. G. (2017) Lanthanide phosphine oxide complexes. *Coordination Chemistry Reviews, 340*, 62-78. *doi*:10.1016/j.ccr.2016.09.012.

Pollmann, K., Kutschke, S., Matys, S., Raff, J., Hlawacek, G., & Lederer, F. L. (2018). Bio-recycling of metals: Recycling of technical products using biological applications. *Biotechnology Advances, 36*:4, 1048-1062. *doi:*10.1016/j.biotechadv.2018.03.006

Sarikaya, M., Tamerler, C., Schwartz, D. T., & Baneyx, F. (2004). Materials assembly and formation using engineered polypeptides. *Annual Review of Materials Research, 34*, 373–408. *doi*:10.1146/annurev.matsci.34.040203.121025

Seker, U. O. S., & Demir, H.V. (2011). Material Binding Peptides for Nanotechnology. *Molecules, 16*, 1426–1451. *doi*:10.3390/molecules16021426

Seredin, V. V., & Dai, S. (2012). Coal deposits as potential alternative sources for lanthanides and yttrium. *International Journal of Coal Geology, 94*, 67-93. *doi*:10.1016/j.coal.2011.11.001.

Smith, G.P., & Scott, J.K. (1993). Libraries of peptides and proteins displayed on filamentous phage. *Methods in Enzymology, 217*, 228–257. *doi*:10.1016/0076-6879(93)17065-D.

Statista Research Department. (2020, August). Recycling rate of e-waste in Germany 2009-2018 [PDF file]. Retrieved from https://www.statista.com/statistics/632731/e-waste-recycling-germany/#:~:text=Recycling%20rate%20of%20e%2Dwaste%20in%20Germany%202009%2D2018&text=Germany's%20recycling%20rate%20of%20electrical,decreased%20in%20the%20following%20years

Tierney, A. N., & Atema, J. (1988). Amino acid chemoreception: effects of pH on receptors and stimuli. *Journal of Chemical Ecology, 14*(1), 135-141. *doi:*10.1007/bf01022537

Zhang, K., Kleit, A. N., & Nieto, A. (2017). An economics strategy for criticality – Application to rare earth element Yttrium in new lighting technology and its sustainable availability. *Renewable and Sustainable Energy Reviews, 77*, 899-915. *doi*:10.1016/j.rser.2016.12.127

Yang, J., Retegan, T., Steenari, B., & Ekberg, C. (2016). Recovery of indium and yttrium from Flat Panel Display waste using solvent extraction. *Separation and Purification Technology, 166*, 117-124. *doi*:10.1016/j.seppur.2016.04.021